International Journal of Bifurcation and Chaos, Vol. 24, No. 2 (2014) 1450015 (23 pages)

DOI: 10.1142/S0218127414500151

Potential Function in a Continuous Dissipative Chaotic System: Decomposition Scheme and Role of Strange Attractor

Yian Ma*
Department of Computer Science and Engineering, Shanghai Jiao Tong University, Shanghai 200240, P. R. China

Qijun Tan†
School of Mathematical Sciences, Fudan University, Shanghai 200433, P. R. China

Ruoshi Yuan
Shanghai Center for Systems Biomedicine, Shanghai Jiao Tong University, Shanghai 200240, P. R. China

Bo Yuan
Department of Computer Science and Engineering, Shanghai Jiao Tong University, Shanghai 200240, P. R. China
boyuan@sjtu.edu.cn

Ping Ao
Shanghai Center for Systems Biomedicine and Department of Physics, Shanghai Jiao Tong University, Shanghai 200240, P. R. China
aoping@sjtu.edu.cn

Received February 25, 2013; Revised October 18, 2013

We demonstrate, first in literature, that potential functions can be constructed in a continuous dissipative chaotic system and can be used to reveal its dynamical properties. To attain this aim, a Lorenz-like system is proposed and rigorously proved chaotic for exemplified analysis. We explicitly construct a potential function monotonically decreasing along the system's dynamics, revealing the structure of the chaotic strange attractor. The potential function is not unique for a deterministic system. We also decompose the dynamical system corresponding to a curl-free structure and a divergence-free structure, explaining for the different origins of chaotic attractor and strange attractor. Consequently, reasons for the existence of both chaotic nonstrange attractors and nonchaotic strange attractors are discussed within current decomposition framework.

Keywords: Dissipative dynamical systems; chaotic attractor; strange attractor.

*Current Address: Department of Applied Mathematics, University of Washington, Seattle, WA 98195, USA.
†Current Address: Department of Mathematics, Penn State University, University Park, PA 16803, USA.

1. Introduction

Nonlinear dynamical systems are known for their complex behaviors: nonpointwise attractor, quasi-periodic oscillation, and chaotic motion [Strogatz, 2001]. These behaviors largely restrict traditional techniques from analyzing the systems globally. We draw inspiration from potential functions in physics. We find a continuous scalar function (and name it potential function) in phase space, monotonically decreasing along the system's dynamics. When the system reaches steady states (i.e. attractor), the scalar function will remain constant. This potential function not only generalizes existing approaches of Lyapunov function and first integral, but also encompasses concepts like stability [Lyapunov, 1992] and reversibility [Li *et al.*, 2010; Vollmer *et al.*, 1998] into a unified framework.

Previously, we have rigorously defined potential function in mathematical terms and demonstrated that potential functions (or Lyapunov functions) can be analytically constructed in oscillating systems [Zhu *et al.*, 2006; Ma *et al.*, 2013]. In this paper, we further motivate such research by showing the construction of potential functions in a chaotic system, and providing additional insights for chaotic and strange attractors.

Constructing potential-like functions in chaotic systems is an approach already taken by researchers. There are various efforts addressing the issue of finding functions with a restricted portion of the properties held by potential functions. There are generalized Hamiltonian approach [Sira-Ramirez & Cruz-Hernandez, 2001], energy-like function technique [Sarasola *et al.*, 2005], minimum action method [Zhou & Weinan, 2010], and etc., in search for a unified description of chaotic dynamics. These previous methods all construct a potential-like function to analyze some chaotic system such as the Lorenz system [Lorenz, 1963]. The scalar functions in these works all lack certain important properties (cf. Sec. 6).

Those important drawbacks of the existing methods motivate a real potential function to describe the behavior of chaotic systems. We organize the paper as follows to demonstrate the construction and application of this potential function. First of all, we formally define the potential function and a decomposition framework in Sec. 2. In Sec. 3, we create an attractor that is chaotic according to the standard definition for analysis. Then, a potential function for this chaotic attractor is constructed in Sec. 4, showing the structure of the chaotic strange attractor. In Sec. 7, we demonstrate that our decomposition framework separates the original vector field into two orthogonal components: a gradient part and a rotation part. This decomposition helps understand the different origins for chaotic attractor and strange attractor, explaining why there exists both chaotic nonstrange attractors and nonchaotic strange attractors.

2. Potential Function

We first state the definition of a potential function. In Sec. 2.1, a decomposition scheme of generic dynamical systems associated with the potential function will be discussed.

Definition 2.1 (Potential Function [Ao, 2004; Yuan *et al.*, 2011]). Suppose a vector field $\dot{\mathbf{x}} = \mathbf{f}(\mathbf{x}) : \mathbb{R}^n \to \mathbb{R}^n$ induces a flow ϕ_t. Let $\Psi : \mathbb{R}^n \to \mathbb{R}$ be a continuous function with derivative: $\dot{\Psi}(\mathbf{x}) = d\Psi/dt|_{\mathbf{x}}$ exist at $\mathbf{x} \in \mathbb{R}^n$. Then Ψ satisfying the following conditions is called a potential function for the dynamical system: $\dot{\mathbf{x}} = \mathbf{f}(\mathbf{x})$.

(a) $\dot{\Psi}(\mathbf{x}) = d\Psi/dt|_{\mathbf{x}} \leq 0$ for all $\mathbf{x} \in \mathbb{R}^n$.
(b) $\dot{\Psi}(\mathbf{x}^*) = 0$ if and only if $\mathbf{x}^* \in \mathcal{O}$, where $\mathcal{O}$ is the limit set of the dynamical system: $\dot{\mathbf{x}} = \mathbf{f}(\mathbf{x})$.

In other words, a potential function is a Lyapunov function. In Definition 2.1, the flow ϕ_t on the limit set $\mathcal{O}$ can be fixed, periodic, or chaotic.

It is proved in [Ma *et al.*, 2013] that: if a trajectory is dense in the limit set, then a locally positive definite Lyapunov function implies asymptotic orbital stability to the trajectory. And by the LaSalle invariance principle, the convergence region can be extended to a bounded simply-connected region: $R = \{\mathbf{x} \,|\, \Psi(\mathbf{x}) < M\}$, satisfying: $\Psi(\mathbf{x})$ is differentiable and $\Psi(\mathbf{x}) < 0$ for any $\mathbf{x} \in R \backslash \mathcal{O}$.

Hence, with the potential function, all the hidden attractors [Leonov & Kuznetsov, 2013] can be found by identifying the local minima of the potential function (an interesting example of hidden attractor is found by [Leonov *et al.*, 2011]).

2.1. *Decomposition scheme*

Previously, we have found that a generic dynamical system can be decomposed into a dissipative component and a conservative component [Yuan & Ao, 2012]:

$$\dot{\mathbf{x}} = \mathbf{f}(\mathbf{x}) = -D(\mathbf{x})\nabla\Psi(\mathbf{x}) + Q(\mathbf{x})\nabla\Psi(\mathbf{x}), \quad (1)$$

where $D(\mathbf{x})$ is a semi-positive definite symmetric matrix and $Q(\mathbf{x})$ is skew-symmetric. Once we obtained the potential function for the system, we can express the two matrices as [Yuan *et al.*, 2011]:

$$D = -\frac{\mathbf{f}\cdot\nabla\Psi}{\nabla\Psi\cdot\nabla\Psi}I \quad (2)$$

and

$$Q = \frac{\mathbf{f}\times\nabla\Psi}{\nabla\Psi\cdot\nabla\Psi}. \quad (3)$$

Here, I denotes identity matrix and the generalized cross product of two vectors defines a matrix: $\mathbf{x}\times\mathbf{y} = A = (a_{ij})_{n\times n} = (x_i y_j - x_j y_i)_{n\times n}$.

For this construction, $(Q\nabla\Psi(\mathbf{x}))\cdot\nabla\Psi = 0$ and $(D\nabla\Psi(\mathbf{x}))\times\nabla\Psi = 0$ (for an arbitrary matrix D, the second relation may not be true), corresponding exactly to the curl-free component and divergence-free component in Helmholtz decomposition [Kobe, 1986]. This means that a generic system is composed of a gradient part and a rotation part [Ao *et al.*, 2013; Qian, 2013]. For the gradient part, potential Ψ is an energy function; for the rotation part, Ψ is a first integral.

Naively, a dynamical system $\dot{\mathbf{x}} = \mathbf{f}(\mathbf{x})$ can always be decomposed into three parts [Cheng *et al.*, 2000]:

$$\dot{\mathbf{x}} = \mathbf{f}(\mathbf{x}) = M(\mathbf{x})\nabla\Psi(\mathbf{x}), \quad (4)$$

$$M(\mathbf{x}) = J(\mathbf{x}) - D(\mathbf{x}) + Q(\mathbf{x}), \quad (5)$$

where $J(\mathbf{x})$ and $D(\mathbf{x})$ are semi-positive definite symmetric matrices and $Q(\mathbf{x})$ is skew-symmetric. In our framework, however, matrix $J(\mathbf{x})$ is zero: $J(\mathbf{x}) = 0$. If we take Ψ as an energy function, $J = 0$ means that in a closed system, energy is either dissipated or conserved, but never created.

Further, as have been discussed in the context of nonequilibrium thermal dynamics [Olson & Ao, 2007], the gradient part and the rotation part correspond to two different structures in geometry: a dissipative bracket $\{\cdot,\cdot\}$; and a generalized Poisson bracket [Arnold *et al.*, 1989] $[\cdot,\cdot]$.[1]

A dissipative bracket $\{\cdot,\cdot\}$ associates with matrix $D(\mathbf{x})$:

$$\{f,g\} = \partial_i f D_{ij}\partial_j g,$$

and is generally defined as symmetric: $\{f,g\} = \{g,f\}$; and semi-positive definite: $\{f,f\} \geq 0$; satisfying Leibniz' rule: $\{fg,h\} = f\{g,h\} + g\{f,h\}$.

While a generalized Poisson bracket $[\cdot,\cdot]$ associates with matrix $Q(\mathbf{x})$:

$$[f,g] = \partial_i f Q_{ij}\partial_j g,$$

and can be generally defined as antisymmetric: $[f,g] = -[g,f]$; satisfying Leibniz' rule: $[fg,h] = f[g,h] + g[f,h]$.

Hence, the original differential equations can be expressed as:

$$\dot{x}_i = -\{x_i,\Psi\} + [x_i,\Psi].$$

That is, a generic dynamical system is a direct composition of the two well-studied geometric structures.

Later, this gradient-rotation decomposition framework would provide additional insight to the understanding of chaotic attractors and strange attractors.

3. Simplified Geometric Lorenz Attractor

Many efforts have been made to analyze the Lorenz system [Lorenz, 1963] as a typical model for chaos [Li *et al.*, 2012]. Yet to the best knowledge of the authors, there is only numerical evidence that the Lorenz equations support a robust strange attractor [Tucker, 1999]. Total understanding of the Lorenz attractor, including but not limited to an analytic proof that the Lorenz attractor is chaotic is still lacking [Smale, 1998].

An early work [Guckenheimer & Williams, 1979] attempted to study chaotic systems by constructing a geometric model in a piecewise fashion to resemble the Lorenz system. The resultant "geometric Lorenz attractor" from the piecewise model is studied in some depth and an analogy is made between it and the Lorenz system [Tucker, 1999]. This methodology is practically effective, yet the model system can become even simpler to be analytically proved as chaotic.

Hence, we start out constructing a simplified geometric Lorenz attractor. The model system is

[1]To avoid confusion, we restrict the use of generalized Poisson brackets in this section (Sec. 2).

described by piecewise continuous ordinary differential equations (ODE), similar to the "geometric Lorenz attractor". We integrate trajectories in each continuous region of the model system. Then we reveal the structure of the attractor by finding the Poincaré map between the continuous regions. Through the Poincaré map, the attractor is proved to be a chaotic attractor according to the widely applied definition [Robinson, 2004] of Devaney chaos.

3.1. *Model system description*

The piecewise continuous ODE model is described in each continuous region (from R_A to R_C, along with $R_{B'}$ and $R_{C'}$ as the symmetric counterparts of R_B and R_C) as follows, corresponding to Fig. 1.

(1) In region R_A, where $x \in [0,2]$,[2] $y \in [-2,2]$, $z \in [0,2]$, $yz \in [-2,2]$:

$$\begin{cases} \dot{x} = 0 \\ \dot{y} = y \\ \dot{z} = -z. \end{cases} \tag{6}$$

The dynamics in this region is characterized by saddle points at $y = z = 0$. These saddle points are responsible for causing bifurcation in originally closed trajectories.

(2) Region R_B is defined as: $x \in [0, 2/3 + 8/(3\pi)) \times \theta]$, $y \in (2,4]$, $z \in [0,2]$, $\sqrt{(z-2)^2 + (y-2)^2} \in [1,2]$, where:

$$\theta = \arccos \frac{y-2}{\sqrt{(z-2)^2 + (y-2)^2}},$$

denoting the angle that point (y,z) form with respect to the center $(2,2)$.
In R_B:

$$\begin{cases} \dot{x} = -\dfrac{x}{\theta + \dfrac{\pi}{4}} \\ \dot{y} = 2 - z \\ \dot{z} = y - 2. \end{cases} \tag{7}$$

Trajectories in this region rotate for an angle of $\pi/2$ with respect to $y = z = 2$ and contract in the x direction.

(3) In region R_C, where $x \in [0, 2/3]$, $y \in [-1,4]$, $z > 2$, $\sqrt{(z-2)^2 + (y-2)^2} \geq 1$,

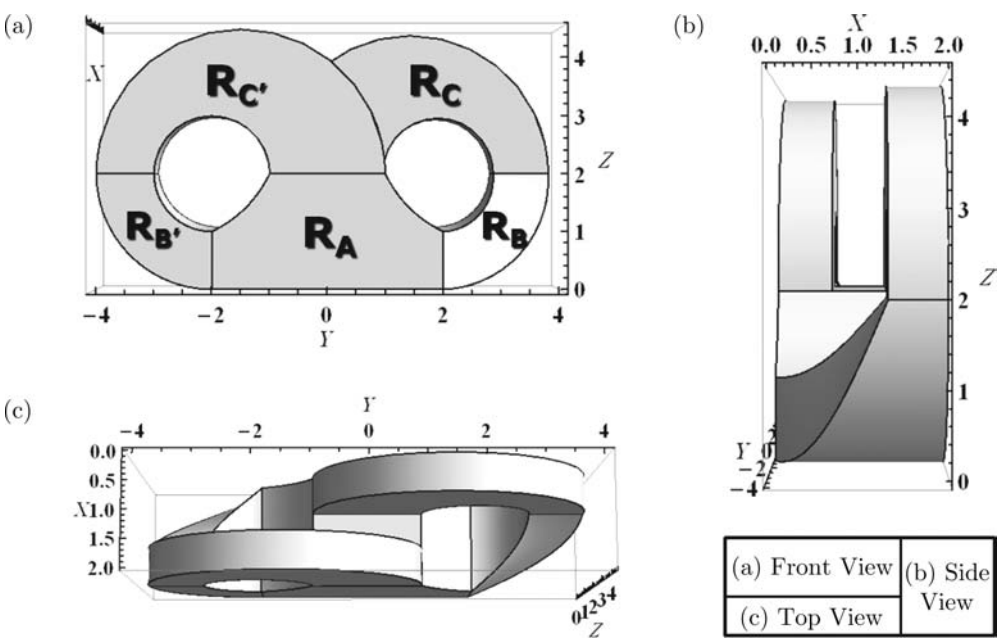

Fig. 1. The Simplified Geometric Lorenz Attractor. The dynamical system we study here is defined piecewise in regions R_A, R_B, and R_C, along with regions $R_{B'}$ and $R_{C'}$ as the symmetric counterparts of R_B and R_C. The front, side, and top views of the regions of definition are shown in panels (a) through (c) respectively. Trajectories of this dynamical system would converge into an attractor $\mathbb{A}_L$ (cf. Sec. 3.4 and Fig. 7), which is a simplified version of the geometric Lorenz attractor.

[2]The square brackets in this (Sec. 3) and the following sections mean closed intervals, not the generalized Poisson brackets.

$\sqrt{(z-2)^2+(y-3/2)^2} \le 5/2$:

$$\begin{cases} \dot{x} = 0 \\ \dot{y} = 2 - z \\ \dot{z} = \dfrac{9y}{8} - \dfrac{21}{8} + \dfrac{\sqrt{(3y-7)^2 + 8(z-2)^2}}{8}. \end{cases} \tag{8}$$

In this region, trajectories rotate for another angle of π with respect to $y = z = 2$ and expand in the y direction.

The whole system is set symmetrical with respect to the line: $x = 1$; $y = 0$; $z \in \mathbb{R}$. We change the coordinate of (x, y, z) into $(2 - x, -y, z)$ to have expressions of the vector field in regions $R_{B'}$ and $R_{C'}$ from expressions in regions R_B and R_C.

(4) Region $R_{B'}$ is defined as: $x \in [4/3 - 8/(3\pi) \times \theta, 2], y \in [-4, -2), z \in [0, 2], \sqrt{(z-2)^2 + (y+2)^2} \in [1, 2]$, where:

$$\theta = \arccos \frac{-y-2}{\sqrt{(z-2)^2 + (y+2)^2}},$$

denoting the angle that point (y, z) form with respect to the center $(-2, 2)$.
In $R_{B'}$:

$$\begin{cases} \dot{x} = \dfrac{2-x}{\theta + \dfrac{\pi}{4}} \\ \dot{y} = z - 2 \\ \dot{z} = -y - 2. \end{cases} \tag{9}$$

Vector field in region $R_{B'}$ corresponds exactly to that in R_B.

(5) In region $R_{C'}$, where $x \in [4/3, 2]$, $y \in [-4, 1]$, $z > 2$, $\sqrt{(z-2)^2 + (y+2)^2} \ge 1$, $\sqrt{(z-2)^2 + (y+3/2)^2} \le 5/2$:

$$\begin{cases} \dot{x} = 0 \\ \dot{y} = z - 2 \\ \dot{z} = -\dfrac{9y}{8} - \dfrac{21}{8} + \dfrac{\sqrt{(3y+7)^2 + 8(z-2)^2}}{8}. \end{cases} \tag{10}$$

Vector field in region $R_{C'}$ corresponds exactly to that in region R_C.

We note that the model system in regions $R_{B'}$ and $R_{C'}$ is just a change of variables of the system in regions R_B and R_C. To avoid redundancy, we will only take regions R_A, R_B and R_C to represent all the regions of definition in the following analysis.

3.2. *Near saddle-focus fixed points*

We have constructed the model system containing one saddle fixed point. As in the Lorenz system, there would actually be another two saddle-focus fixed points when the system expands to the whole $\mathbb{R}^3$ space. In this section, we complete the dynamical system near the two saddle-focus fixed points so that the convergence behavior away from the attractor can be further demonstrated.

We denote the regions near the two saddle-focus fixed points as regions R_D and $R_{D'}$ (cf. Fig. 2), each consisting of three parts. For region R_D, we denote the three parts as: regions R_{D^A}, R_{D^B}, and R_{D^C}. Regions R_D and $R_{D'}$ are symmetrical with respect to the line: $x = 1$; $y = 0$; $z \in \mathbb{R}$, just as in the previous section. Hence, we follow the convention stated in the previous section: to take regions $R_{D^{A'}}$, $R_{D^{B'}}$, and $R_{D^{C'}}$ representing their symmetrical counterparts. The regions: R_{D^A}, R_{D^B}, and R_{D^C} and the differential equations in them are written as the following.

(1) Region R_{D^A} is close to region R_A and is defined as: $x \in [0, 2]$, $y \in [1, 2]$, $z \in [1, 2]$, $yz \in (2, 4]$. We simply take differential dynamical system in it to be the same as that in region R_A:

$$\begin{cases} \dot{x} = 0 \\ \dot{y} = y \\ \dot{z} = -z. \end{cases} \tag{11}$$

States in this region are unstable in the y direction and stable in the z direction, causing a rotation effect.

(2) Region R_{D^B} is close to region R_B and is defined as: $x \in [0, 2/3 + 8/(3\pi) \times \theta]$, $y \in (2, 3]$, $z \in [1, 2]$, $\sqrt{(z-2)^2 + (y-2)^2} < 1$.
Here,

$$\theta = \arccos \frac{y-2}{\sqrt{(z-2)^2 + (y-2)^2}},$$

denoting the angle that point (y, z) form with respect to the center $(2, 2)$.

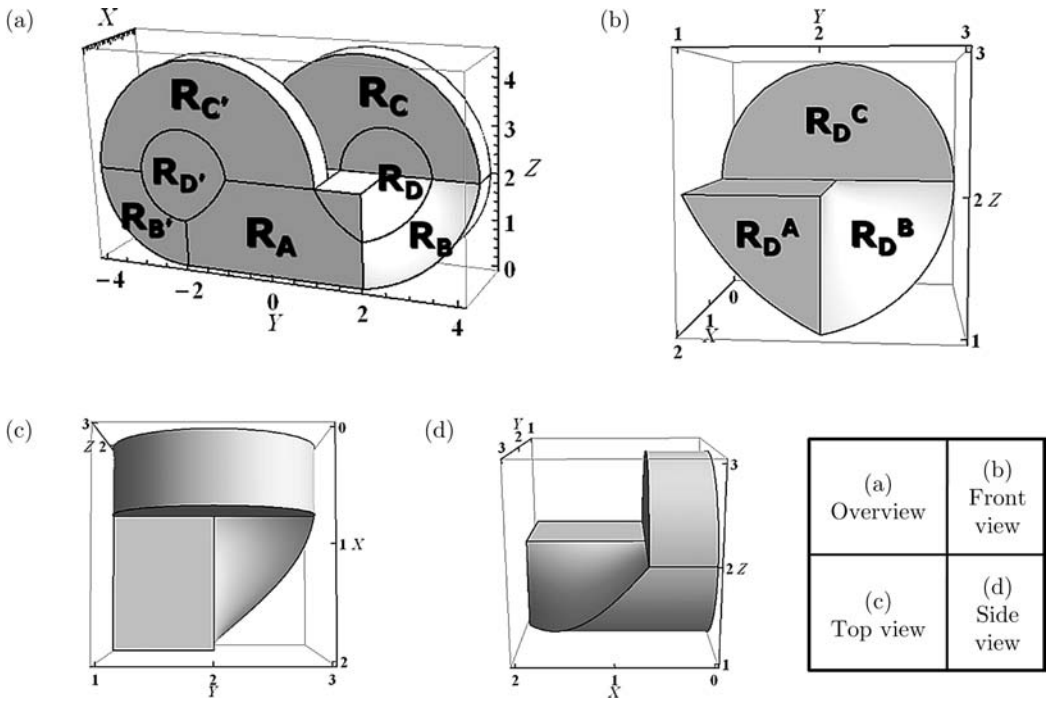

Fig. 2. Near Saddle-Focus Fixed Points. When the system expands to contain regions R_D and $R_{D'}$, two saddle-focus fixed points would emerge. This figure elaborates on the system near the two saddle-focus fixed points. (a) The regions containing the two saddle-focus fixed points, i.e. R_D and $R_{D'}$ are shown along with other regions. (b)–(d) The front, top, and side views of region R_D are shown respectively.

In region R_{DB}:

$$\begin{cases} \dot{x} = -\dfrac{x}{\theta + \dfrac{\pi}{4}} \\ \dot{y} = 2 - z \\ \dot{z} = y - 2. \end{cases} \tag{12}$$

Same as in region R_B, trajectories in this region rotate for an angle of $\pi/2$ with respect to $y = z = 2$ and contract in the x direction.

(3) In region R_{DC}, where $x \in [0, 2/3]$, $y \in [1, 3]$, $z > 2$, $\sqrt{(z-2)^2 + (y-2)^2} < 1$:

$$\begin{cases} \dot{x} = 0 \\ \dot{y} = 2 - z + (y-2) \\ \qquad \times \left(\dfrac{1}{\sqrt{(z-2)^2 + (y-2)^2}} - 1 \right) \\ \dot{z} = y - 2 + (z-2) \\ \qquad \times \left(\dfrac{1}{\sqrt{(z-2)^2 + (y-2)^2}} - 1 \right). \end{cases} \tag{13}$$

In this region, trajectories tend to converge to the unit-radius circle centered at $y = z = 2$. Hence, states in the whole region R_D are attracted to the circle: $x = 0$, $\sqrt{(z-2)^2 + (y-2)^2} = 1$.

It is observable that region R_D containing a saddle-focus fixed point, forms a semi-stable limit cycle at $x = 0$, $\sqrt{(z-2)^2 + (y-2)^2} = 1$ (when y, $z \in [1, 2]$, the curve of the limit cycle changes expression to: $x = 0$, $yz = 2$). This limit cycle locates at the boundaries between region R_D and its adjacent regions. This phenomenon corresponds with many observations that fixed points transit into chaotic behaviors through limit cycles [Zhou & Weinan, 2010].

Also, this section demonstrates that the domain of definition in the model system is not restricted to the regions discussed above. If we take dynamical system in the rest of $\mathbb{R}^3$ space converging into the defined regions (R_A through R_D, $R_{B'}$ through $R_{D'}$), the domain of definition can be expanded to the whole space.

3.3. *Trajectory and Poincaré map*

Based on Eqs. (5)–(9), we simulate the trajectory of the dynamical system (shown in Fig. 3). Trajectories in each region can be analytically solved. To study the structure of the attractor, we solve

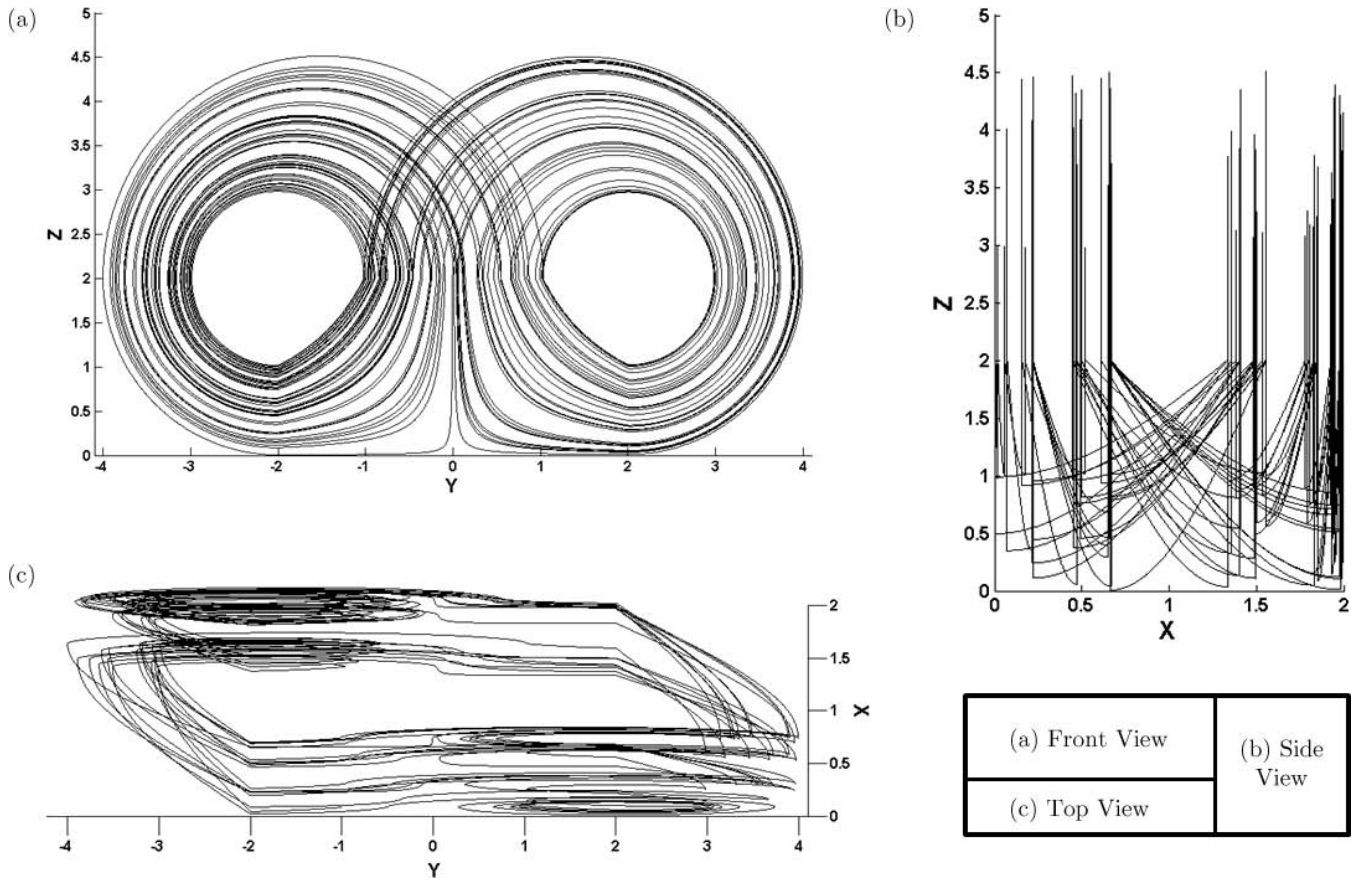

Fig. 3. Simulated Trajectory of the System. We simulated a trajectory of the dynamical system constructed. It appears to have "erratic" behaviors, similar to the Lorenz system.

the trajectories in regions R_A, R_B, and R_C respectively:

(1) In region R_A, trajectories are represented as:

$$\begin{cases} x = x_0 \\ y = y_0 e^t \\ z = z_0 e^{-t}, \end{cases} \tag{14}$$

where z_0 can usually be taken as 2.

Hence, states in this region are exponentially unstable in the y direction and exponentially stable in the z direction.

(2) In region R_B, trajectories are:

$$\begin{cases} x = x_0\left(1 - \dfrac{4}{3\pi}t\right) \\ y = \sqrt{(y_0-2)^2 + (z_0-2)^2}\sin t + 2 \\ z = -\sqrt{(y_0-2)^2 + (z_0-2)^2}\cos t + 2, \end{cases} \tag{15}$$

where y_0 can be 2.

Parameter t increases from 0 to $\pi/2$, and we can observe that $x(t)$ decreases monotonically while $y(t)$ and $z(t)$ form a circle.

(3) In region R_C, trajectories are:

$$\begin{cases} x = x_0 \\ y = \sqrt{\left(\dfrac{3}{2}y_0 - \dfrac{7}{2}\right)^2 + (z_0-2)^2}\cos t \\ \qquad + \dfrac{1}{3}\left(1 - \sqrt{\left(\dfrac{3}{2}y_0 - \dfrac{7}{2}\right)^2 + (z_0-2)^2}\right) + 2 \\ z = \sqrt{\left(\dfrac{3}{2}y_0 - \dfrac{7}{2}\right)^2 + (z_0-2)^2}\sin t + 2, \end{cases} \tag{16}$$

where z_0 can be 2.

As t increases from 0 to π, trajectories in region R_C move along circles determined by initial conditions.

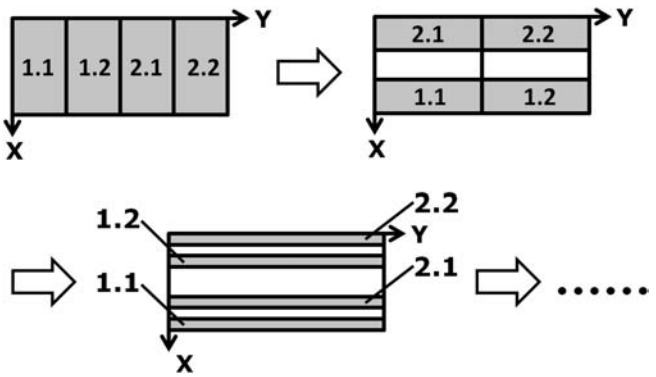

Fig. 4. Poincaré Map of the Dynamical System. This Poincaré map is taken over the surface of $z = 2$. This map is a "baker's map" and creates a Cantor set multiplying a real line segment.

To further study the structure of the attractor of the system, we want to calculate the Poincaré map of the system. Here, we take the Poincaré surface of section as: $z = 2$, and find the resultant Poincaré map as a discrete dynamical system defined on $[0, 2] \times [-1, 1]$ (shown in Fig. 4 and follows).

When $(x, y) \in [0, 2] \times [0, 1]$,

$$\begin{cases} x_{n+1} = \dfrac{1}{3} x_n \\ y_{n+1} = 2y_n - 1; \end{cases} \tag{17}$$

When $(x, y) \in [0, 2] \times [-1, 0)$,

$$\begin{cases} x_{n+1} = \dfrac{1}{3} x_n + \dfrac{4}{3} \\ y_{n+1} = 2y_n + 1. \end{cases} \tag{18}$$

The above discrete dynamical system is a "baker's map" [Kuznetsov, 2012], and can be understood figuratively as the following. In the x direction, the mapping is contractive. The square of definition: $[0, 2] \times [-1, 1]$ is contracted to the one third of it, forming a rectangle: $[0, 2/3] \times [-1, 1]$. In the y direction, the mapping is expansive just as the doubling map [Robinson, 2004]. The rectangle is stretched to: $[0, 2/3] \times [-3, 1]$. Then we keep the right half of the resulting rectangle and move the left half: $[0, 2/3] \times [-3, -1)$ to the position: $[0, 2/3] \times [-1, 1)$. It can readily be seen that the invariant set is formed by iteratively removing the middle third of the intervals along the x direction.

3.4. *Attractor of the model system*

We denote the attractor of the model system as: $\mathbb{A}_L$. And with the Poincaré map of the model system defined as a dynamical system on $[0, 2] \times [-1, 1]$ [Eqs. (17) and (18)], we denote its attractor as: $\mathbb{A}_P$. In this section, we first express attractor $\mathbb{A}_P$ of the Poincaré map in terms of the Cantor set; then we can describe attractor $\mathbb{A}_L$ of the original model system.

Here, an attractor $\mathbb{A}$ of a dynamical system with flow ϕ_t can be formally defined as the following.

Definition 3.1 (Attractor). An attractor $\mathbb{A}$ of a dynamical system $\dot{\mathbf{x}} = \mathbf{f}(\mathbf{x})$ with flow ϕ_t is a compact invariant set, with an open set U containing $\mathbb{A}$ such that for each $\mathbf{x} \in U$, $\phi_t(\mathbf{x}) \in U$ for all $t \geq 0$ and $\mathbb{A} = \bigcap_{t \geq 0} \phi_t(U)$.

We have already found the Poincaré map of the model system by iteratively removing the middle third of the invariant sets along the x direction. That is, first, remove the set $(2/3, 4/3) \times [-1, 1]$; then, remove the middle third of the left two sets $[0, 2/3] \times [-1, 1]$ and $[4/3, 2] \times [-1, 1]$; and iterate the process all along. We represent all the removed intervals iteratively as the following:

$$\mathbb{C}_1 = \left(\frac{2}{3}, \frac{4}{3}\right) \times [-1, 1]$$

and

$$\mathbb{C}_{n+1} = \left(\frac{\mathbb{C}_n}{3} \cup \frac{\mathbb{C}_n + 4}{3}\right) \times [-1, 1]. \tag{19}$$

The attractor of the Poincaré map is $[0, 2] \times [-1, 1]$ minus the union of all the sets $\mathbb{C}_i$:

$$\begin{aligned} \mathbb{A}_P &= [0, 2] \times [-1, 1] - \bigcup_{i=1}^{\infty} \mathbb{C}_i \times [-1, 1] \\ &= \left([0, 2] - \bigcup_{i=1}^{\infty} \mathbb{C}_i\right) \times [-1, 1] \\ &= \mathbb{C} \times [-1, 1], \end{aligned} \tag{20}$$

where $\mathbb{C}$ denotes the Cantor set [Peitgen *et al.*, 2004] defined on the interval of $[0, 2]$.

Attractor $\mathbb{A}_P$ of the Poincaré map is the Cantor set multiplying a real line segment. We can calculate its box-counting dimension [Peitgen *et al.*, 2004]

to be:

$$d_b(\mathbb{A}_P) = \liminf_{\epsilon\to 0} \frac{\log N(\epsilon, \mathbb{A}_P)}{\log\left(\frac{1}{\epsilon}\right)}$$

$$= 1 + \frac{\ln(2)}{\ln(3)}. \quad (21)$$

Here, we consider subdivision of $\mathbb{R}^n$ into boxes of sides of length ϵ. And $N(\epsilon, \mathbb{A}_P)$ denotes the number of ϵ-boxes needed to cover the attractor $\mathbb{A}_P$ (a more elaborate definition can be found in [Robinson, 1995]). According to the calculation, attractor $\mathbb{A}_P$ is of fractal dimension, a strange attractor [Anishchenko & Strelkova, 1998].

With the trajectories of the system analytically solved in each region, we further express attractor $\mathbb{A}_L$ of the model system as (assuming $\theta = \arccos(y-2)/\sqrt{(z-2)^2+(y-2)^2}$):

In region R_A, $x \in \mathbb{C}$;
In region R_B, $(4/(3\pi) \times \theta + 1/3)^{-1} x \in \mathbb{C}$;
In region R_C, $x \in \mathbb{C}$.

The box-counting dimension of attractor $\mathbb{A}_L$ is then calculated to be:

$$d_b(\mathbb{A}_L) = \liminf_{\epsilon\to 0} \frac{\log N(\epsilon, \mathbb{A}_L)}{\log\left(\frac{1}{\epsilon}\right)}$$

$$= 2 + \frac{\ln(2)}{\ln(3)}. \quad (22)$$

The attractor $\mathbb{A}_L$ of the model system is hence a strange attractor with fractal dimension.

It will also be proved in the following Sec. 3.5 that attractors $\mathbb{A}_P$ and $\mathbb{A}_L$ are chaotic attractors.

3.5. *Proof of the attractor as chaotic*

By the widely applied definition [Robinson, 2004] of Devaney chaos, an attractor $\mathbb{A}$ is defined as a chaotic attractor if:

(1) the attractor is indecomposable (i.e. if $\emptyset \neq \mathbb{A}' \subseteq \mathbb{A}$ is an attractor, then $\mathbb{A}' = \mathbb{A}$);
(2) the system is sensitive to initial conditions when restricted to $\mathbb{A}$ (defined in the following Definition 3.2).

Definition 3.2. A map (a continuous-time system is defined similarly) has sensitive dependence on initial conditions when restricted to its invariant set $\mathbb{A}$, if there exists r, for any $p_0 \in \mathbb{A}$, and $\delta > 0$, there exists $p_0' \in \mathbb{A}$: $|p_0' - p_0| < \delta$, and an iterate $k > 0$ such that

$$|f^k(p_0') - f^k(p_0)| \geq r. \quad (23)$$

Attractor $\mathbb{A}_L$ has already been taken as the smallest attracting set, so it is an indecomposable attractor by default. We just need to prove that the system has sensitive dependence on initial conditions when restricted to $\mathbb{A}_L$.

We first prove that attractor $\mathbb{A}_P$ of the Poincaré map is chaotic using the fact that the doubling map [Robinson, 2004] is sensitively dependent upon initial conditions when restricted to its attractor. Then we prove in exactly the same way that attractor $\mathbb{A}_L$ of the model system is chaotic by the sensitivity of $\mathbb{A}_P$.

Proposition 1 [Sensitive Dependence of the Poincaré Map]. *The Poincaré map of the model system has sensitive dependence upon initial conditions when restricted to its attractor $\mathbb{A}_P$.*

Proof. For any $p_0 \in \mathbb{A}_P$, with its neighboring initial point $p_0' \in \mathbb{A}_P$, we take p_0' as $(x_0', y_0') = (x_0', y_0' - \delta \cdot \mathrm{Sign}(y_0))$.

Clearly, $\|p_n - p_n'\| \geq |y_n - y_n'|$. So, proving sensitivity to initial conditions of $\mathbb{A}_P$ is equivalent to that of the Doubling Map:

$$y_{n+1} = \lfloor 2y_n \rfloor, \quad (y_i \in (0,1), \forall\, i). \quad (24)$$

With the sensitive dependence upon initial conditions of doubling map when restricted to its attractor proved [Robinson, 2004], Poincaré map of the model system is also sensitive when restricted to its attractor $\mathbb{A}_P$. ■

In exactly the same way, the model system can thus be proved sensitively dependent upon initial conditions when restricted to its attractor $\mathbb{A}_L$. Hence, it is a chaotic attractor by definition.

We also calculate the commonly used indicator of chaos: Lyapunov exponents [Robinson, 2004] for the model system at fixed points. By solving the Lyapunov exponents in each coordinate direction, we find that in region R_A: $\ell_x = 0$, $\ell_y = 1$, and $\ell_z = -1$. It can be found that there is a positive Lyapunov exponent $\ell_y = 1$ denoting exponential expansion in the y direction. In regions R_B and R_C, $\ell_x = \ell_y = \ell_z = 0$, which means that the expansion effect causing the sensitivity of the system is mainly exerted in region R_A.

Here, the Lyapunov exponents are calculated to demonstrate that the mixing effect is imposed by the saddle dynamics at the center; while other parts of the system facilitate recurrence, an interesting phenomenon observed in the Lorenz system. It should be noted that in time varying systems, positive largest Lyapunov exponent may not guarantee chaoticity [Leonov & Kuznetsov, 2007; Leonov, 2008].

From this and the former section, we find that the attractor of the model system is a chaotic attractor with fractal dimension: a strange chaotic attractor [Anishchenko & Strelkova, 1998].

4. Construction of Potential Function in the Chaotic System

Based on the above observation, we want to start constructing a potential function to describe the overall structure of the chaotic system. First, we construct a "seed function", $\mathcal{F}$, to account for the "strangeness" of the system's attractor. Then we prove its continuous differentiability so that it can be applied in the construction of potential function for the model system. Later, we explicitly express the potential function in terms of the seed function $\mathcal{F}$.

4.1. *Definition of the "seed function" $\mathcal{F}$*

Definition 4.1 [Function $\mathcal{F}$]. Let

$$f_1(x) = \begin{cases} 0, & x \in \left[0, \frac{2}{3}\right] \cup \left[\frac{4}{3}, 2\right] \\ 1 - \cos(3\pi x), & x \in \left(\frac{2}{3}, \frac{4}{3}\right); \end{cases} \tag{25}$$

and

$$f_{n+1}(x) = \begin{cases} \frac{1}{9} \times f_n(3x), & x \in \left[0, \frac{2}{3}\right] \\ 0, & x \in \left(\frac{2}{3}, \frac{4}{3}\right) \\ \frac{1}{9} \times f_n(3x-4), & x \in \left[\frac{4}{3}, 2\right]. \end{cases} \tag{26}$$

Thus, we define the function $\mathcal{F}(x)$ as:

$$\mathcal{F}(x) = \sum_{n=1}^{\infty} f_n(x). \tag{27}$$

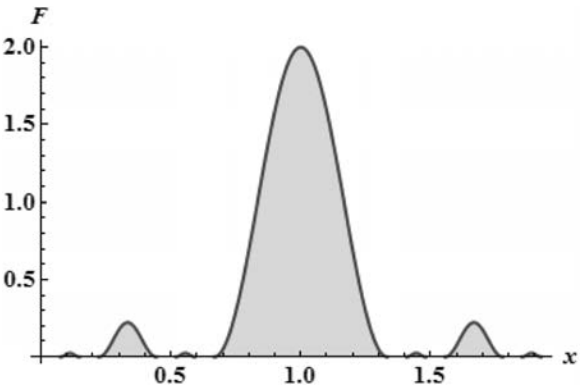

Fig. 5. Illustration of the Self-Similar Function: $\mathcal{F}$. We hereby plot function $\mathcal{F}$ to intuitively visualize it. With $\mathcal{F}$, construction of a potential function in the chaotic system would be natural.

Function $\mathcal{F}(x)$ defined on $[0, 2]$ is shown in Fig. 5. It has a fractal structure as the attractor $\mathbb{A}_P$ of the Poincaré map.

4.2. *Proof of $\mathcal{F}(x)$ as continuous differentiable*

In this subsection, we prove that the function $\mathcal{F}(x)$ defined by Eq. (27) is continuously differentiable.

Proposition 2 [Continuous Differentiability of Function $\mathcal{F}$]. *Function $\mathcal{F}(x) = \sum_{n=1}^{\infty} f_n(x)$ defined in Definition 4.1 is continuously differentiable.*

Proof. We first calculate the derivative of every $f_n(x)$ on $[0, 2]$. Then we bound $f_n(x)$ and $|f_n'(x)|$ by geometric series to prove uniform convergence of their sums, thus proving that $\mathcal{F}(x) = \sum_{n=1}^{\infty} f_n(x)$ is continuously differentiable.

By definition [Eqs. (25) and (26)]:

$$f_1(x) = \begin{cases} 0, & x \in \left[0, \frac{2}{3}\right] \cup \left[\frac{4}{3}, 2\right] \\ 1 - \cos(3\pi x), & x \in \left(\frac{2}{3}, \frac{4}{3}\right) \end{cases}$$

and

$$f_{n+1}(x) = \begin{cases} \frac{1}{9} \times f_n(3x), & x \in \left[0, \frac{2}{3}\right] \\ 0, & x \in \left(\frac{2}{3}, \frac{4}{3}\right) \\ \frac{1}{9} \times f_n(3x-4), & x \in \left[\frac{4}{3}, 2\right], \end{cases}$$

taking derivative on both sides:

$$f_1'(x) = \begin{cases} 0, & x \in \left[0, \frac{2}{3}\right] \cup \left[\frac{4}{3}, 2\right] \\ 3\pi \sin(3\pi x), & x \in \left(\frac{2}{3}, \frac{4}{3}\right) \end{cases}$$

and

$$f_{n+1}'(x) = \begin{cases} \frac{1}{3} \times f_n'(3x), & x \in \left[0, \frac{2}{3}\right] \\ 0, & x \in \left(\frac{2}{3}, \frac{4}{3}\right) \\ \frac{1}{3} \times f_n'(3x-4), & x \in \left[\frac{4}{3}, 2\right]. \end{cases}$$

We can see that $f_1(x) \leq 2$ and $|f_1'(x)| \leq 3\pi$. And also, $f_n'(x)$ is continuous for any $x \in [0, 2]$.

If we further denote the set in which $f_n(x)$ is nonzero as $\mathbb{C}_n$, we have:

$$\mathbb{C}_1 = \left(\frac{2}{3}, \frac{4}{3}\right)$$

and

$$\mathbb{C}_{n+1} = \frac{\mathbb{C}_n}{3} \cup \frac{\mathbb{C}_n + 4}{3}. \tag{28}$$

Since $\mathbb{C}_n \subset [0, 2]$,

$$\frac{\mathbb{C}_n}{3} \cap \frac{\mathbb{C}_n + 4}{3} \subset \left[0, \frac{2}{3}\right] \cap \left[\frac{4}{3}, 2\right] = \emptyset.$$

We thus can conclude that:

$$f_{n+1}(x) \leq \frac{1}{9} f_n(x) \leq 9^{-n} f_1(x) \leq 2 \times 9^{-n}$$

and

$$|f_{n+1}'(x)| \leq \frac{1}{3}|f_n'(x)| \leq 3^{-n}|f_1'(x)| \leq 3\pi \times 3^{-n},$$

for any $x \in [0, 2]$.

At this point, we give an upper bound for the series $\sum_{n=1}^{m} f_n(x)$ and its derivative (although the least upper bound is even smaller if we note that $\mathbb{C}_n \cap \mathbb{C}_{n+1}$ is actually empty, an upper bound is good enough):

$$\sum_{n=1}^{m} f_n(x) \leq \frac{9}{4} - \frac{1}{4} \times 9^{-m},$$

and that

$$\sum_{n=1}^{m} |f_n'(x)| \leq \frac{9\pi}{2} - \frac{3\pi}{2} \times 3^{-m}.$$

$\sum_{n=1}^{m} f_n(x)$ is uniformly convergent and $\sum_{n=1}^{\infty} f_n'(x)$ is uniformly absolutely-convergent. Therefore, $\sum_{n=1}^{\infty} f_n'(x)$ and $\sum_{n=1}^{\infty} f_n(x)$ are all uniformly convergent.

With every $f_n(x)$ continuously differentiable, $\mathcal{F}(x) = \sum_{n=1}^{\infty} f_n(x)$ is continuously differentiable:

$$\frac{d}{dx}\mathcal{F}(x) = \sum_{n=1}^{\infty} f_n'(x). \tag{29}$$

■

Clearly, the points where $\mathcal{F}(x) = \mathcal{F}'(x) = 0$ form a Cantor set $\mathbb{C}$ corresponding to the attractor $\mathbb{A}_L$ of the model system ($\mathcal{F}(x) = 0$ if and only if $x \in \mathbb{C}$). At this point, we found that the potential function can be constructed in the following section.

4.3. *Constructing potential function in the chaotic system*

As in Eq. (12) we use θ to denote the angle that (y, z) form with respect to the center $(2, 2)$:

$$\theta = \arccos \frac{y-2}{\sqrt{(z-2)^2 + (y-2)^2}}.$$

Then, we construct potential function in each region respectively:

(1) In the right part of region R_A, where $x, y, z \in [0, 2]$, $yz \in [-2, 2]$:

$$\Psi_A = \left(\frac{4}{9\pi}\theta + \frac{5}{9}\right)\mathcal{F}(x). \tag{30}$$

(2) In region R_B, where $x \in [0, 2]$, $y \in (2, 4]$, $z \in [0, 2]$, $\sqrt{(z-2)^2 + (y-2)^2} \in [1, 2]$:

$$\Psi_B = \left(\frac{4}{9\pi}\theta + \frac{5}{9}\right)\mathcal{F}\left(\left(\frac{4}{3\pi}\theta + \frac{1}{3}\right)^{-1} x\right). \tag{31}$$

(3) In region R_C, where $x \in [0, 2/3]$, $y \in [-2, 4]$, $z > 2$, $\sqrt{(z-2)^2 + (y-2)^2} \geq 1$, $\sqrt{(z-2)^2 + (y-3/2)^2} \leq 5/2$:

$$\Psi_C = \left(-\frac{4}{9\pi}\theta + \frac{5}{9}\right)\mathcal{F}(3x). \tag{32}$$

We plot the potential function taken on the Poincaré section in Fig. 6.

If we are also interested in the dynamics near saddle-focus fixed points, the potential function in regions R_{D^A}, R_{D^B}, and R_{D^C} can also be constructed as follows.

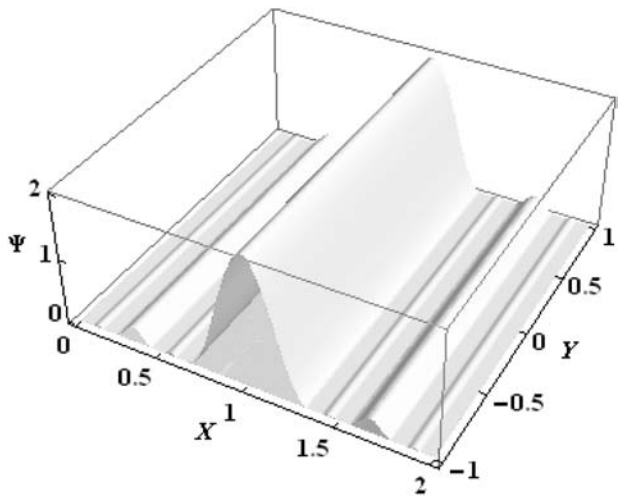

Fig. 6. Potential Function on Poincaré Section. On the Poincaré section, the potential function is demonstrated to be a fractal object: it is zero when point $(x, y, 2)$ belongs to the attractor $\mathbb{A}_L$, i.e. $\Psi|_{z=2} = 0$ when $x \in \mathbb{C}$. And when $(x, y, 2)$ does not belong to the attractor, the potential function Ψ has a self-similar structure.

(1) In region R_{D^A}, where $x \in [0, 2]$, $y \in [1, 2]$, $z \in [1, 2]$, $yz \in [2, 4]$:

$$\Psi_{D^A} = \left(\frac{4}{9\pi}\theta + \frac{5}{9}\right)\mathcal{F}(x) + 1 - \left(\frac{1}{2}yz - 2\right)^2. \tag{33}$$

(2) In region R_{D^B}, where $x \in [0, 2/3 + 8/(3\pi) \times \theta]$, $y \in [2, 3]$, $z \in [1, 2]$, $\sqrt{(z-2)^2 + (y-2)^2} \in [0, 1]$:

$$\Psi_{D^B} = \left(\frac{4}{9\pi}\theta + \frac{5}{9}\right)\mathcal{F}\left(\left(\frac{4}{3\pi}\theta + \frac{1}{3}\right)^{-1} x\right) + 1 - (z-2)^2 - (y-2)^2. \tag{34}$$

(3) In region R_{D^A}, where $x \in [0, 2/3]$, $y \in [1, 3]$, $z > 2$, $\sqrt{(z-2)^2 + (y-2)^2} \leq 1$:

$$\Psi_{D^C} = \left(-\frac{4}{9\pi}\theta + \frac{5}{9}\right)\mathcal{F}(3x) + 1 - (z-2)^2 - (y-2)^2. \tag{35}$$

Potential function in region R_D is gradually higher in the center of the region than in its boundary with other regions. Hence, points in this region will naturally converge to its boundary (at $x = 0, \sqrt{(z-2)^2 + (y-2)^2} = 1$, when $y > 2$ or $z > 2$; and at $x = 0, yz = 2$, when $y, z \in [1, 2]$).

The construction of the potential function is not unique. If we change the expression of $f_1(x)$ in the definition of the "seed function" $\mathcal{F}(x)$, we can have a different potential function for the system.

5. Verification of the Potential Function

In this section, we verify the integrity of the potential function from three angles: First, we show that it is continuous in the domain. Second, we demonstrate that it decreases monotonically along the vector field. Third, we show that $\nabla\Psi(x) = 0$ if and only if x belongs to the attractor of the system.

5.1. *Continuity of the potential function*

(1) At the boundary of region R_A and R_B, $y = 2$, $x \in [0, 2]$, $z \in [0, 1]$.

Substituting values of x, y, z into Eq. (30), $\theta = \arccos 0 = \pi/2$; $(4/(3\pi) \times \theta + 1/3)^{-1} = 1$; and $(4/(9\pi) \times \theta + 5/9) = 7/9$. Therefore,

$$\Psi_A|_{y=2^-} = \frac{7}{9}\mathcal{F}(x) = \Psi_{B_1}|_{y=2^+}.$$

(2) At the boundary of region R_B and R_C, $z = 2$, $x \in [0, 2/3]$, and $y \in [3, 4]$.

Substituting values of x, y, z into Eq. (31), $\theta = \arccos 1 = 0$; $(4/(3\pi) \times \theta + 1/3)^{-1} = 3$; and $(\pm 4/(9\pi) \times \theta + 5/9) = 5/9$. Therefore,

$$\Psi_B|_{z=2^-} = \frac{5}{9}\mathcal{F}(3x) = \Psi_{C_1}|_{z=2^+}.$$

(3) At the boundary of region R_C and R_A, $z = 2$, $x \in [0, 2/3]$, and $y \in [-1, 1]$.

Substituting values of x, y, z into Eq. (32), $\theta = \arccos(-1) = \pi$; $(4/(9\pi) \times \theta + 5/9) = 1$; and $(-4/(9\pi) \times \theta + 5/9) = 1/9$. Therefore,

$$\Psi_A|_{z=2^-} = \mathcal{F}(x) \quad \Psi_C|_{z=2^+} = \frac{1}{9}\mathcal{F}(3x).$$

It can be observed that in the definition of $\mathcal{F}(x) = \sum_{n=1}^{\infty} f_n(x)$,

$$f_{n+1}(x) = \frac{1}{9}f_n(3x), \quad x \in \left[0, \frac{2}{3}\right].$$

Because $f_1(x) = 0$ in $[0, 2/3]$,

$$\frac{1}{9}\mathcal{F}(3x) = \sum_{n=2}^{\infty} f_n(x) = \mathcal{F}(x), \tag{36}$$

for $x \in [0, 2/3]$.

Please note that this is a critical point in the construction of potential function in cases of self-similar attractors. If the potential function constructed is not self-similar accordingly, the boundary would not totally fit.

5.2. *Monotonic decreasing of the potential function*

In this subsection, we take Lie derivative (derivative along the vector field) [Arnold, 1983] of the potential function along vector fields in each region remembering that $\mathcal{F}(x) \geq 0$ for any $x \in [0, 2]$.

(1) In the right part of region R_A, where $x, y, z \in [0, 2]$, $yz \in [-2, 2]$:

$$\begin{cases} \dot{x} = 0 \\ \dot{\theta} = \mathrm{Sgn}(z-2)\left(-\dfrac{z-2}{(z-2)^2+(y-2)^2}\dot{y} + \dfrac{y-2}{(z-2)^2+(y-2)^2}\dot{z}\right) = -\dfrac{(2-y)z+(2-z)y}{(z-2)^2+(y-2)^2}. \end{cases}$$

Since $\dot{x} = 0$ and $y, z \in [0, 2]$,

$$\dot{\Psi}_A = \frac{4}{9\pi}\mathcal{F}(x)\dot{\theta} = -\frac{4}{9\pi}\frac{(2-y)z+(2-z)y}{(z-2)^2+(y-2)^2}\mathcal{F}(x) \leq 0. \tag{37}$$

(2) In region R_B, where $x \in [0, 2]$, $y \in (2, 4]$, $z \in [0, 2]$, $\sqrt{(z-2)^2+(y-2)^2} \in [1, 2]$:

$$\begin{cases} \dot{x} = -x\left(\dfrac{\pi}{4} + \arccos\dfrac{y-2}{\sqrt{(z-2)^2+(y-2)^2}}\right)^{-1} = -x\left(\dfrac{\pi}{4}+\theta\right)^{-1} \\ \dot{\theta} = \dfrac{z-2}{(z-2)^2+(y-2)^2}\dot{y} - \dfrac{y-2}{(z-2)^2+(y-2)^2}\dot{z} = -1. \end{cases}$$

$$\begin{aligned} \dot{\Psi}_B &= \frac{4}{9\pi}\mathcal{F}\left(\left(\frac{4}{3\pi}\theta+\frac{1}{3}\right)^{-1}x\right)\dot{\theta} + \left(\frac{4}{9\pi}\theta+\frac{5}{9}\right)\left(\frac{4}{3\pi}\theta+\frac{1}{3}\right)^{-2}\mathcal{F}'\left(\left(\frac{4}{3\pi}\theta+\frac{1}{3}\right)^{-1}x\right) \\ &\quad\times\left(\left(\frac{4}{3\pi}\theta+\frac{1}{3}\right)\dot{x} - \frac{4}{3\pi}x\dot{\theta}\right) \\ &= -\frac{4}{9\pi}\mathcal{F}\left(\left(\frac{4}{3\pi}\theta+\frac{1}{3}\right)^{-1}x\right) + \left(\frac{4}{9\pi}\theta+\frac{5}{9}\right)\left(\frac{4}{3\pi}\theta+\frac{1}{3}\right)^{-2}\mathcal{F}'\left(\left(\frac{4}{3\pi}\theta+\frac{1}{3}\right)^{-1}x\right) \\ &\quad\times\left(-\left(\frac{4}{3\pi}\theta+\frac{1}{3}\right)\left(\frac{\pi}{4}+\theta\right)^{-1}x + \frac{4}{3\pi}x\right). \end{aligned}$$

Since $(-(\frac{4}{3\pi}\theta+\frac{1}{3})(\frac{\pi}{4}+\theta)^{-1}x + \frac{4}{3\pi}x) = 0$,

$$\dot{\Psi}_B = -\frac{4}{9\pi}\mathcal{F}\left(\left(\frac{4}{3\pi}\theta+\frac{1}{3}\right)^{-1}x\right) \leq 0. \tag{38}$$

(3) In region R_C, where $x \in [0, 2/3]$, $y \in [-1, 4]$, $z > 2$, $\sqrt{(z-2)^2+(y-2)^2} \geq 1$, $\sqrt{(z-2)^2+(y-3/2)^2} \leq 5/2$:

$$\begin{cases} \dot{x} = 0 \\ \dot{\theta} = -\dfrac{z-2}{(z-2)^2+(y-2)^2}\dot{y} + \dfrac{y-2}{(z-2)^2+(y-2)^2}\dot{z} \\ \quad = \dfrac{(z-2)^2}{(z-2)^2+(y-2)^2} + \dfrac{y-2}{(z-2)^2+(y-2)^2}\left(\dfrac{9y}{8} - \dfrac{21}{8} + \dfrac{\sqrt{(3y-7)^2+8(z-2)^2}}{8}\right) > 0. \end{cases}$$

Hence,

$$\dot{\Psi}_C = -\frac{4}{9\pi}\mathcal{F}(3x)\dot{\theta} \le 0. \tag{39}$$

5.3. *Potential function and the attractor*

In this subsection, we verify that the potential function attains extremum: $\nabla\Psi(\mathbf{x}) = 0$ if and only if $\mathbf{x} = (x, y, z)$ belongs to the attractor $\mathbb{A}_L$ of the system. Again, $\theta = \arccos(y-2)/\sqrt{(z-2)^2+(y-2)^2}$.

(1) In the right part of region R_A, where $x, y, z \in [0, 2]$, $yz \in [-2, 2]$:

$$\nabla\Psi_A = \begin{pmatrix} \left(\frac{4}{9\pi}\theta + \frac{5}{9}\right)\mathcal{F}'(x) \\ \frac{4}{9\pi}\frac{z-2}{(z-2)^2+(y-2)^2}\mathcal{F}(x) \\ -\frac{4}{9\pi}\frac{y-2}{(z-2)^2+(y-2)^2}\mathcal{F}(x) \end{pmatrix}.$$

In this equation, $\mathcal{F}(x) = 0$ and $\mathcal{F}'(x) = 0$ if and only if $x \in \mathbb{C}$; and point (x, y, z) belongs to the attractor $\mathbb{A}_L$ if and only if $x \in \mathbb{C}$. Combining the two equivalence relations, $\nabla\Psi_A = 0$ if and only if $(x, y, z) \in \mathbb{A}_L$.

(2) In region R_B, where $x \in [0, 2]$, $y \in (2, 4]$, $z \in [0, 2]$, $\sqrt{(z-2)^2+(y-2)^2} \in [1, 2]$:

$$\nabla\Psi_B = \begin{pmatrix} \left(\frac{4}{9\pi}\theta + \frac{5}{9}\right)\left(\frac{4}{3\pi}\theta + \frac{1}{3}\right)^{-1}\mathcal{F}'\left(\left(\frac{4}{3\pi}\theta + \frac{1}{3}\right)^{-1}x\right) \\ \frac{4}{9\pi}\frac{z-2}{(z-2)^2+(y-2)^2} \\ \quad\times\left(\mathcal{F}\left(\left(\frac{4}{3\pi}\theta + \frac{1}{3}\right)^{-1}x\right) - \left(\frac{4}{3\pi}\theta + \frac{5}{3}\right)\left(\frac{4}{3\pi}\theta + \frac{1}{3}\right)^{-2}\mathcal{F}'\left(\left(\frac{4}{3\pi}\theta + \frac{1}{3}\right)^{-1}x\right)\right) \\ -\frac{4}{9\pi}\frac{y-2}{(z-2)^2+(y-2)^2} \\ \quad\times\left(\mathcal{F}\left(\left(\frac{4}{3\pi}\theta + \frac{1}{3}\right)^{-1}x\right) - \left(\frac{4}{3\pi}\theta + \frac{5}{3}\right)\left(\frac{4}{3\pi}\theta + \frac{1}{3}\right)^{-2}\mathcal{F}'\left(\left(\frac{4}{3\pi}\theta + \frac{1}{3}\right)^{-1}x\right)\right) \end{pmatrix}.$$

In this equation, $\mathcal{F}((4/(3\pi)\times\theta + 1/3)^{-1}x) = 0$ and $\mathcal{F}'((4/(3\pi)\times\theta + 1/3)^{-1}x) = 0$ if and only if $(4/(3\pi)\times\theta + 1/3)^{-1}x \in \mathbb{C}$; and point (x, y, z) belongs to the attractor $\mathbb{A}_L$ if and only if $(4/(3\pi)\times\theta + 1/3)^{-1}x \in \mathbb{C}$. Combining the two equivalence relations, $\nabla\Psi_B = 0$ if and only if $(x, y, z) \in \mathbb{A}_L$.

(3) In region R_C, where $x \in [0, 2/3]$, $y \in [-1, 4]$, $z > 2$, $\sqrt{(z-2)^2+(y-2)^2} \ge 1$, $\sqrt{(z-2)^2+(y-3/2)^2} \le 5/2$:

$$\nabla\Psi_C = \begin{pmatrix} \left(-\frac{4}{3\pi}\theta + \frac{5}{3}\right)\mathcal{F}'(3x) \\ \frac{4}{9\pi}\frac{z-2}{(z-2)^2+(y-2)^2}\mathcal{F}(3x) \\ -\frac{4}{9\pi}\frac{y-2}{(z-2)^2+(y-2)^2}\mathcal{F}(3x) \end{pmatrix}.$$

In this equation, $\mathcal{F}(3x) = 0$ and $\mathcal{F}'(3x) = 0$ if and only if $x \in \mathbb{C}$; and point (x, y, z) belongs to the attractor $\mathbb{A}_L$ if and only if $x \in \mathbb{C}$. Combining the two equivalence relations, $\nabla\Psi_C = 0$ if and only if $(x, y, z) \in \mathbb{A}_L$.

In exactly the same way, we can also show the integrity of the potential function in region R_D.

6. Comparison with Related Works

As discussed in the introduction, constructing a potential-like function in the chaotic system is an effort that is by no means totally strange to researchers. Until recently, there are various efforts seeking to describe chaotic dynamics using generalized Hamiltonian approach [Sira-Ramirez & Cruz-Hernandez, 2001], energy-like function technique [Sarasola *et al.*, 2005], minimum action method [Zhou & Weinan, 2010], and etc. These previous methods all construct a potential-like scalar function to analyze certain chaotic system. Unfortunately, the scalar functions in these works all lack certain important properties.

For example, the generalized Hamiltonian systems approach takes a quadratic form of the state variables as the "generalized Hamiltonian" [Sira-Ramirez & Cruz-Hernandez, 2001], a Hamiltonian that includes conserved dynamics, energy dissipation, and energy input: corresponding to the case of $J(\mathbf{x}) \neq 0$ in Eq. (5). This generalized Hamiltonian increases and decreases along with time and becomes a chaotic oscillating signal itself. Therefore, it remains an issue as to what additional insight this generalized Hamiltonian can provide about the original system.

The energy-like function technique is essentially similar to the generalized Hamiltonian approach. Its energy-like function differs from the generalized Hamiltonian in a way that it may not be a quadratic form of the state variables. Rather, the energy-like function is constructed based on the "geometric appearance" [Sarasola *et al.*, 2005] of the attractor corresponding to the specific chaotic system. Although this technique would seem more sophisticated, its energy-like function still oscillates chaotically along with time, describing chaotic dynamics in a chaotic fashion. Loss of monotonicity restricts the function from describing the system's essential properties like stability and controllability [Sabuco *et al.*, 2012; Guo *et al.*, 2012].

The minimum action method, however, casts the problem under the light of zero noise limit. By constructing an auxiliary Hamiltonian [Freidlin & Wentzell, 2008] (commonly denoted as "Freidlin–Wentzell Hamiltonian"), Freidlin–Wentzell action functional can be minimized [Freidlin & Wentzell, 1998]. This method analyzes the chaotic system by possible transitions between limit sets [Zhou & Weinan, 2010]. But since the Freidlin–Wentzell Hamiltonian can be not bounded even in globally stable systems, it is not a quantitative measure comparable between points in state space, hence, not an ideal potential function.

In short, each of all the previous works focuses on one attribute of the potential function. However, as we can see from our constructive result, only when all the requirements (in Definition 1) are met, would the potential function reflect evolution of the whole system and structure of the chaotic attractor. In this sense, the current work is the first construction to satisfy such strong conditions, providing a both detailed and global description for a chaotic system.

Once such Lyapunov function is obtained, robustness analysis [Sastry, 1999], optimal control [Zinober, 1994], and attractor dimension [Leonov, 2008] problems can be solved straightforwardly.

7. Chaotic Attractor and Strange Attractor

With the potential function constructed, we can solve the system's attractor without any need of numerical simulation. We find that the attractor is composed of connected surfaces, each of infinite layers. Starting from the plane $x = 2$, we show the configuration of these layers in Fig. 7. Since geometric configuration of chaotic attractor interests many researchers [Gilmore, 1998], we demonstrate in the figure that the chaotic attractor of the system studied in this paper consists of orientable surfaces.

The chaotic attractor of the model system in this paper is a strange attractor of fractal dimension [Anishchenko & Strelkova, 1998]. In the literature of dynamical systems, there have long been discussions about the relationship between chaotic attractors and strange attractors [Grebogi *et al.*, 1984]. Several examples of strange nonchaotic attractors and nonstrange chaotic attractors have been found [Anishchenko & Strelkova, 1998]. In recent years, strange nonchaotic attractors have been observed in

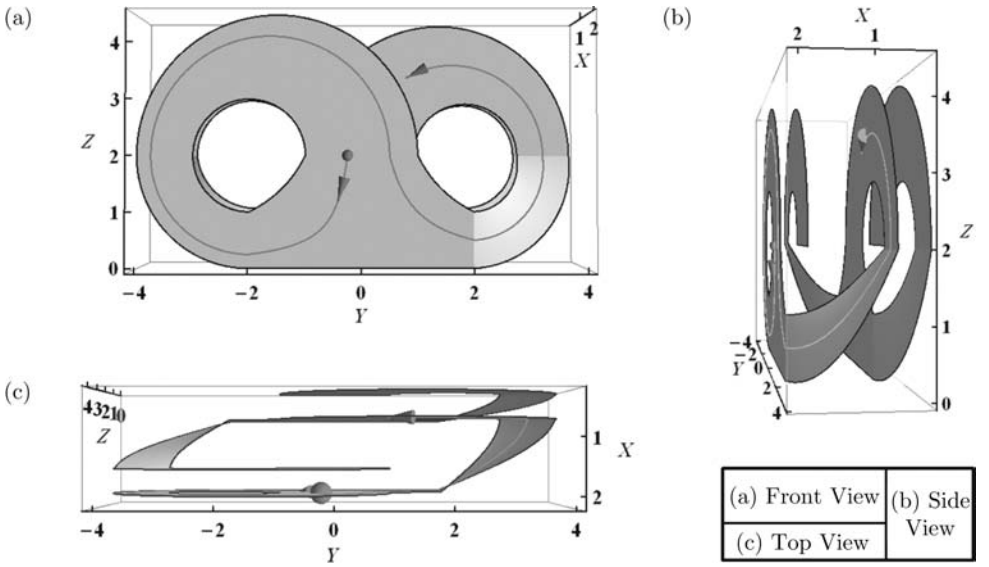

Fig. 7. Strange Chaotic Attractor. We find that a connected surface of the attractor is of infinite layers. We show how surface $x = 2$ is linked to the other equipotential layers. It can be seen that the surface of the attractor is orientable. We hereby demonstrate the strange chaotic attractor viewed from (a) front, (b) side and (c) top. The trajectory running from point (2, 1/4, 2) is also shown in the figure.

a number of diverse experimental situations ranging from quasiperiodically driven mechanical or electronic systems to plasma discharges. And recently, considerable effort has gone into searching for the occurrence of these attractors [Prasad *et al.*, 2007].

The potential function approach provides a unified framework to treat the topics of chaotic attractors and strange attractors together. To illustrate this insight, we need to apply our decomposition method [Eq. (1)]:

$$\dot{\mathbf{x}} = \mathbf{f}(\mathbf{x}) = -D\nabla\Psi(\mathbf{x}) + Q\nabla\Psi(\mathbf{x})$$

where

$$D = -\frac{\mathbf{f}\cdot\nabla\Psi}{\nabla\Psi\cdot\nabla\Psi}I$$

and

$$Q = \frac{\mathbf{f}\times\nabla\Psi}{\nabla\Psi\cdot\nabla\Psi}.$$

We first analyze our model system with this decomposition framework in Sec. 7.1. In Secs. 7.2 and 7.3, we further modify our model system to two typical cases interesting to many researchers: a non-strange chaotic attractor and a strange nonchaotic attractor. After analyzing these two cases, we explain the different origins of chaotic attractors and strange attractors in general in Sec. 7.4.

7.1. *Decomposition of the chaotic system*

According to our decomposition scheme, we first decompose the chaotic dynamical system in each region into two components: the gradient component and the rotation component.

In region R_A, $\nabla\Psi_A$ is solved as:

$$\nabla\Psi_A = \begin{pmatrix} \left(\frac{4}{9\pi}\theta + \frac{5}{9}\right)\mathcal{F}'(x) \\ -\frac{4}{9\pi}\frac{2-z}{(z-2)^2+(y-2)^2}\mathcal{F}(x) \\ \frac{4}{9\pi}\frac{2-y}{(z-2)^2+(y-2)^2}\mathcal{F}(x) \end{pmatrix}.$$

We can find the expression of the matrix D_A, accounting for the gradient component of the vector field in region R_A:

$$D_A = -\frac{\mathbf{f}_A\cdot\nabla\Psi_A}{\nabla\Psi_A\cdot\nabla\Psi_A}I = \frac{\frac{4}{9\pi}\frac{(2-y)z+(2-z)y}{(z-2)^2+(y-2)^2}\mathcal{F}(x)}{\left(\frac{4}{9\pi}\theta+\frac{5}{9}\right)^2(\mathcal{F}'(x))^2 + \frac{\left(\frac{4}{9\pi}\right)^2}{(z-2)^2+(y-2)^2}(\mathcal{F}(x))^2}I. \quad (40)$$

The decomposed gradient part would be:

$$D_A\nabla\Psi_A = \frac{\dfrac{4}{9\pi}\dfrac{(2-y)z+(2-z)y}{(z-2)^2+(y-2)^2}\mathcal{F}(x)}{\left(\dfrac{4}{9\pi}\theta+\dfrac{5}{9}\right)^2(\mathcal{F}'(x))^2+\dfrac{\left(\dfrac{4}{9\pi}\right)^2}{(z-2)^2+(y-2)^2}(\mathcal{F}(x))^2}\begin{pmatrix}\left(\dfrac{4}{9\pi}\theta+\dfrac{5}{9}\right)\mathcal{F}'(x)\\ -\dfrac{4}{9\pi}\dfrac{2-z}{(z-2)^2+(y-2)^2}\mathcal{F}(x)\\ \dfrac{4}{9\pi}\dfrac{2-y}{(z-2)^2+(y-2)^2}\mathcal{F}(x)\end{pmatrix}.$$

Also, we can find the decomposed rotation part by finding Q_A as:

$$\begin{aligned}Q_A &= \frac{\mathbf{f}_A\times\nabla\Psi_A}{\nabla\Psi_A\cdot\nabla\Psi_A}\\ &= \frac{1}{\left(\dfrac{4}{9\pi}\theta+\dfrac{5}{9}\right)^2(\mathcal{F}'(x))^2+\dfrac{\left(\dfrac{4}{9\pi}\right)^2}{(z-2)^2+(y-2)^2}(\mathcal{F}(x))^2}\\ &\quad\times\begin{pmatrix}0 & -y\left(\dfrac{4}{9\pi}\theta+\dfrac{5}{9}\right)\mathcal{F}'(x) & z\left(\dfrac{4}{9\pi}\theta+\dfrac{5}{9}\right)\mathcal{F}'(x)\\ y\left(\dfrac{4}{9\pi}\theta+\dfrac{5}{9}\right)\mathcal{F}'(x) & 0 & -\dfrac{4}{9\pi}\dfrac{(2-z)z-(2-y)y}{(z-2)^2+(y-2)^2}\mathcal{F}(x)\\ -z\left(\dfrac{4}{9\pi}\theta+\dfrac{5}{9}\right)\mathcal{F}'(x) & \dfrac{4}{9\pi}\dfrac{(2-z)z-(2-y)y}{(z-2)^2+(y-2)^2}\mathcal{F}(x) & 0\end{pmatrix}.\end{aligned}\tag{41}$$

The decomposed rotation part would then be:

$$\begin{aligned}Q_A\nabla\Psi_A &= \frac{1}{\left(\dfrac{4}{9\pi}\theta+\dfrac{5}{9}\right)^2(\mathcal{F}'(x))^2+\dfrac{\left(\dfrac{4}{9\pi}\right)^2}{(z-2)^2+(y-2)^2}(\mathcal{F}(x))^2}\\ &\quad\times\begin{pmatrix}-\dfrac{4}{9\pi}\left(\dfrac{4}{9\pi}\theta+\dfrac{5}{9}\right)\dfrac{(y-2)z+(z-2)y}{(z-2)^2+(y-2)^2}\mathcal{F}'(x)\mathcal{F}(x)\\ y\left(\dfrac{4}{9\pi}\theta+\dfrac{5}{9}\right)^2(\mathcal{F}'(x))^2+\left(\dfrac{4}{9\pi}\right)^2\dfrac{(y-2)^2y-(y-2)(z-2)z}{((z-2)^2+(y-2)^2)^2}(\mathcal{F}(x))^2\\ -z\left(\dfrac{4}{9\pi}\theta+\dfrac{5}{9}\right)^2(\mathcal{F}'(x))^2+\left(\dfrac{4}{9\pi}\right)^2\dfrac{(y-2)y(z-2)-(z-2)^2z}{((z-2)^2+(y-2)^2)^2}(\mathcal{F}(x))^2\end{pmatrix}.\end{aligned}\tag{42}$$

As the system approaches its attractor, i.e. $\mathcal{F}(x)\to 0$,

$$\frac{\mathcal{F}(x)}{(\mathcal{F}'(x))^2} = \lim_{x\to 0}\frac{\left(\dfrac{1}{9}\right)^n(1-\cos(3\pi x))}{\left(\left(\dfrac{1}{3}\right)^n 3\pi\sin(3\pi x)\right)^2} = \lim_{x\to 0}\frac{\left(\dfrac{1}{9}\right)^n\dfrac{1}{2}(3\pi x)^2}{\left(\left(\dfrac{1}{3}\right)^n 9\pi^2 x\right)^2} = \frac{1}{18\pi^2}.\tag{43}$$

When the system converges to its attractor, the gradient matrix D_A would be:

$$D_A = -\frac{\frac{4}{9\pi}\frac{(y-2)z+(z-2)y}{(z-2)^2+(y-2)^2}}{\left(\frac{4}{9\pi}\theta+\frac{5}{9}\right)^2}\frac{\mathcal{F}(x)}{(\mathcal{F}'(x))^2}I$$

$$= -\frac{2}{81\pi^3}\frac{\frac{(y-2)z+(z-2)y}{(z-2)^2+(y-2)^2}}{\left(\frac{4}{9\pi}\theta+\frac{5}{9}\right)^2}I, \tag{44}$$

which is finite.

Consequently, the gradient component $D_A\nabla\Psi_A$ of the system would converge to zero when approaching the attractor. Motion on the attractor is caused totally by the rotation part: $Q_A\nabla\Psi_A$.

In exactly the same way, the decomposition procedure can be carried out in region B and region C, and the same conclusion holds.

7.2. *Nonstrange chaotic attractor*

We first examine an example of nonstrange chaotic attractor by modifying our original system a little [in region R_B, Eq. (12)]:

In region R_B, we set

$$\theta = \arccos\frac{y-2}{\sqrt{(z-2)^2+(y-2)^2}},$$

as in Eq. (12). Then we change the dynamical system in region R_B (defined as $x \in [0, 4/\pi \times \theta]$, $y \in [2,4]$, $z \in [0,2]$, $\sqrt{(z-2)^2+(y-2)^2} \in [1,2]$) to:

$$\begin{cases} \dot{x} = -\dfrac{x}{\theta} \\ \dot{y} = 2 - z \\ \dot{z} = y - 2. \end{cases}$$

The same as in the original system, the domain of definition can be expanded to the whole $\mathbb{R}^3$ space.

Consequently, the Poincaré map would be as follows:

When $(x, y) \in [0,2] \times [0,1]$,

$$\begin{cases} x_{n+1} = 0 \\ y_{n+1} = 2y_n - 1. \end{cases}$$

When $(x, y) \in [0,2] \times [-1,0)$,

$$\begin{cases} x_{n+1} = 1 \\ y_{n+1} = 2y_n + 1. \end{cases}$$

The attractor $\mathbb{A}'_L$ of the modified system would be: (assuming $\theta = \arccos(y-2)/\sqrt{(z-2)^2+(y-2)^2}$):

In region R_A, $x = 0$ or 2;
In region R_B, $(\pi/2) \times (x/\theta) = 0$ or 2;
In region R_C, $x = 0$ or 2.

The attractor is shown in Fig. 8. We can calculate its box-counting dimension to be:

$$d_b(\mathbb{A}'_L) = \liminf_{\epsilon\to 0}\frac{\log N(\epsilon, \mathbb{A}'_L)}{\log\left(\frac{1}{\epsilon}\right)} = 2, \tag{45}$$

which is an integer dimension. Actually, the attractor $\mathbb{A}'_L$ is just two orientable surfaces folded together. It is no longer a strange attractor anymore.

Exactly as in the original system, the modified attractor can be proved to be chaotic. And we can also calculate the commonly used indicator of chaos: Lyapunov exponents [Robinson, 2004] for the model system at fixed points. Lyapunov exponents are solved in each direction as: $\ell_x = 0$, $\ell_y = 1$, and $\ell_z = -1$ in region R_A (in other regions, $\ell_x = \ell_y = \ell_z = 0$). It is found that there is a positive Lyapunov exponent $\ell_y = 1$ denoting exponential expansion in the y direction, exactly as in the original model system.

The modified attractor is a nonstrange chaotic attractor.

Now, we construct a potential function Φ for the new dynamical system by first appointing a new seed function $F(x)$ defined in $[0,2]$:

$$F(x) = 1 - \cos(\pi x), \quad x \in [0,2].$$

The potential function can be represented in terms of F as:

(1) In the right part of region R_A, where $x, y, z \in [0,2]$:

$$\Phi_A = \left(\frac{\theta}{\pi}\right)F(x).$$

(2) In region R_B, where $y \in [2,4]$, $z \in [0,2]$, $\sqrt{(z-2)^2+(y-2)^2} \in [1,2]$, $x \in [0, 4/\pi \times \theta]$:

$$\Phi_B = \left(\frac{\theta}{\pi}\right)F\left(\frac{\pi x}{2\theta}\right).$$

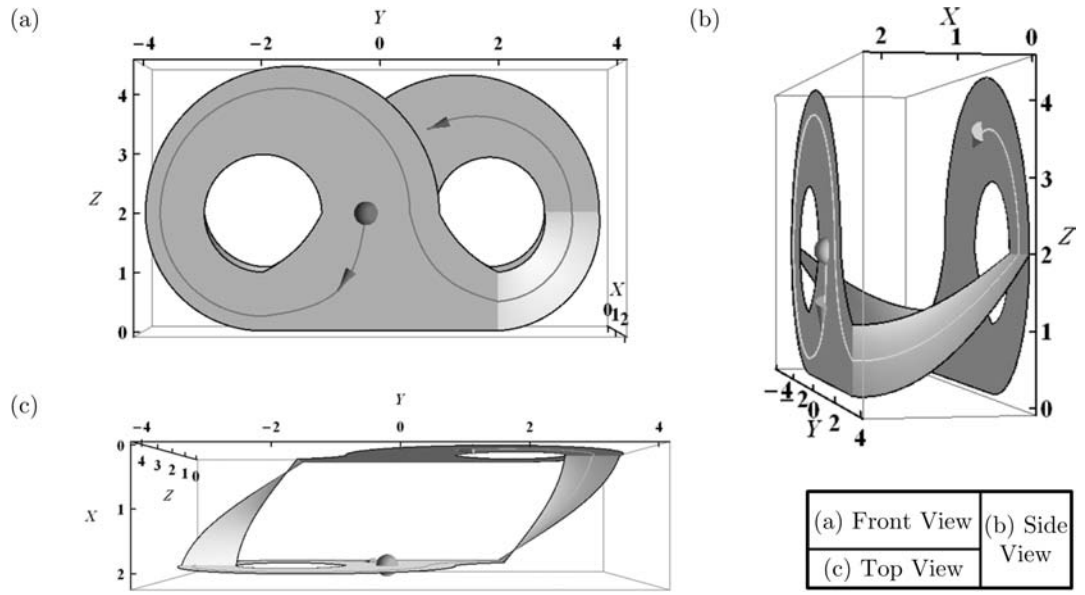

Fig. 8. Nonstrange Chaotic Attractor. We change the expression of the system a little, so that the attractor is just two orientable surfaces folded together, rather than a fractal structure. However, it remains to be a chaotic attractor. We hereby demonstrate the nonstrange chaotic attractor viewed from (a) front, (b) side and (c) top. The trajectory running from point (2, 1/4, 2) is also shown in the figure.

(3) In region R_C, where $x = 2$, $y \in [-2, 4]$, $z > 2$, $\sqrt{(z-2)^2 + (y-2)^2} \geq 1$, $\sqrt{(z-2)^2 + (y-3/2)^2} \leq 5/2$:

$$\Phi_C = 0.$$

For the potential function Φ defined above, $\{(x, \theta) \,|\, \Phi(x, \theta) = 0\}$ corresponds to the attractor. We can further decompose the system as we did with the original model system:

$$\dot{\mathbf{x}} = \mathbf{f}(\mathbf{x}) = -D\nabla\Phi(\mathbf{x}) + Q\nabla\Phi(\mathbf{x}).$$

In region R_A:

$$\nabla\Phi_A = \frac{1}{\pi}\begin{pmatrix} \theta F'(x) \\ -\dfrac{2-z}{(z-2)^2 + (y-2)^2}F(x) \\ \dfrac{2-y}{(z-2)^2 + (y-2)^2}F(x) \end{pmatrix}. \tag{46}$$

$$D_A = -\frac{\mathbf{f}_A \cdot \nabla\Phi_A}{\nabla\Phi_A \cdot \nabla\Phi_A} I = \frac{\pi\dfrac{(2-y)z + (2-z)y}{(z-2)^2 + (y-2)^2}F(x)}{\theta^2(F'(x))^2 + \dfrac{1}{(z-2)^2 + (y-2)^2}(F(x))^2} I.$$

The decomposed gradient part would be:

$$D_A\nabla\Phi_A = \frac{\dfrac{(2-y)z + (2-z)y}{(z-2)^2 + (y-2)^2}F(x)}{\theta^2(F'(x))^2 + \dfrac{(F(x))^2}{(z-2)^2 + (y-2)^2}} \begin{pmatrix} \theta F'(x) \\ -\dfrac{2-z}{(z-2)^2 + (y-2)^2}F(x) \\ \dfrac{2-y}{(z-2)^2 + (y-2)^2}F(x) \end{pmatrix}. \tag{47}$$

By calculating Q_A:

$$Q_A = \frac{\mathbf{f}_A \times \nabla\Phi_A}{\nabla\Phi_A \cdot \nabla\Phi_A}$$
$$= \frac{\pi}{\theta^2(F'(x))^2 + (F(x))^2} \begin{pmatrix} 0 & -y\theta F'(x) & z\theta F'(x) \\ y\theta F'(x) & 0 & -\dfrac{(2-z)z-(2-y)y}{(z-2)^2+(y-2)^2}F(x) \\ -z\theta F'(x) & \dfrac{(2-z)z-(2-y)y}{(z-2)^2+(y-2)^2}F(x) & 0 \end{pmatrix}, \tag{48}$$

the decomposed rotation part would be:

$$Q_A \nabla\Phi_A = \frac{\pi}{\theta^2(F'(x))^2 + (F(x))^2} \begin{pmatrix} -\dfrac{(y-2)z+(z-2)y}{(z-2)^2+(y-2)^2}\theta F'(x)F(x) \\ y\theta^2(F'(x))^2 + \dfrac{(y-2)^2y-(y-2)(z-2)z}{((z-2)^2+(y-2)^2)^2}(F(x))^2 \\ -z\theta^2(F'(x))^2 + \dfrac{(y-2)y(z-2)-(z-2)^2z}{((z-2)^2+(y-2)^2)^2}(F(x))^2 \end{pmatrix}. \tag{49}$$

The properties of the gradient part and the rotation part correspond exactly to the original model system. That is, the gradient part converges to zero when approaching the attractor; motion on the attractor is determined by the rotation part.

7.3. *Strange nonchaotic attractor*

A strange nonchaotic attractor can also be constructed.

We simply take the gradient of potential function Ψ of the original system in each region of definition:

$$\begin{cases} \dot{x} = -\partial_x\Psi \\ \dot{y} = -\partial_y\Psi \\ \dot{z} = -\partial_z\Psi. \end{cases}$$

If we take the left part of region R_A for example, the vector field would be:

$$\mathbf{f}_A = \begin{pmatrix} -\left(\dfrac{4}{9\pi}\theta + \dfrac{5}{9}\right)\mathcal{F}'(x) \\ -\dfrac{4}{9\pi}\dfrac{z-2}{(z-2)^2+(y-2)^2}\mathcal{F}(x) \\ \dfrac{4}{9\pi}\dfrac{y-2}{(z-2)^2+(y-2)^2}\mathcal{F}(x) \end{pmatrix}.$$

The resultant ODE system defined by the gradient is dynamical since it is Lipschitz continuous in each region. And with the existence and uniqueness of the flow guaranteed by Lipschitz continuity, conditions for the system being a dynamical system can be satisfied and extended to include boundaries.

The system would converge downward the potential function Ψ until reaching the states where $\Psi = 0$. Consequently, the attractor of this system is characterized by $\Psi = 0$, as in the original model system. Hence, the gradient system's attractor is the same attractor $\mathbb{A}_L$ of the original model system, whose box-counting dimension:

$$d_b(\mathbb{A}_L) = \liminf_{\epsilon\to 0} \frac{\log N(\epsilon, \mathbb{A}_L)}{\log\left(\dfrac{1}{\epsilon}\right)} = 2 + \frac{\ln(2)}{\ln(3)}. \tag{50}$$

The system has a strange attractor.

Since $\nabla\Psi = 0$ when $\Psi = 0$, the dynamical system is not sensitively dependent upon initial conditions when restricted to the attractor. The attractor is not chaotic. Also, its Lyapunov exponents at the fixed points (where $x \in \mathbb{C}$, $y = z = 0$) would be: $\ell_x = -(1/3)^n \times 9\pi^2$, $\ell_y = \ell_z = 0$. Hence, it is a strange nonchaotic attractor.

Decomposition of this system would give: $D(\mathbf{x}) = I$ and $Q(\mathbf{x}) = 0$. Thus, $\mathbf{f}(\mathbf{x}) = -D\nabla\Psi(\mathbf{x})$ is just the gradient system.

7.4. *Chaotic attractor versus strange attractor*

The previous two examples show that the concepts of chaotic attractor and strange attractor do not imply each other. Under our framework of decomposition [Eq. (1)]:

$$\dot{\mathbf{x}} = \mathbf{f}(\mathbf{x}) = -D\nabla\Psi(\mathbf{x}) + Q\nabla\Psi(\mathbf{x}).$$

Since $\dot{\Psi} = \nabla\Psi \cdot \dot{\mathbf{x}} = \nabla\Psi \cdot (D\nabla\Psi)$, Ψ decreases monotonically according to the gradient component $D\nabla\Psi$ of the vector field f. Then the attractor is naturally characterized by: $\{\mathbf{x}^* \,|\, D\nabla\Psi(\mathbf{x}^*) = 0\}$. So, whether the attractor is a strange attractor is determined by the gradient part of the vector field.

Sensitive dependence upon initial conditions when restricted to the attractor, however, is determined by the rotation part of the vector field: $Q\nabla\Psi$. Once the system has evolved to the limit set, $D\nabla\Psi$ would equal to zero, and $Q\nabla\Psi$ would be prevalent. Hence, the rotational vector field on the attractor causes the traverse motion on the limit set, leading to dynamical sensitivity [Liao, 2012]. In this sense nonzero rotation part of the dynamical system is a necessary condition for causing hyperbolic chaos [Kuznetsov, 2012].

By observing Eq. (1), we can find the following scenarios:

When Ψ is a simple potential function, i.e. a Morse function, the system only contains fixed points. This type of dynamics is well understood [Marsden & McCracken, 1976].

When Ψ is not a Morse function, in particular, when $\nabla\Psi(\mathbf{x}) = 0$ on a connected fractal surface, the system's dynamics become complicated. In this case, if:

(1) Q is bounded on the attractor, i.e. $Q\nabla\Psi = 0$, and D is not zero, the system's attractor is strange, but there is no motion on the attractor. We have a strange nonchaotic attractor. Dynamic behavior near such attractor is dominated by the gradient part;
(2) $Q\nabla\Psi \neq 0$ on the attractor, and D is uniformly zero in the whole space, the system is characterized by conserved dynamics. The attractor would be the whole state space, and hence, nonstrange. But chaotic motion still exists in this situation, corresponding to the previous observation of Hamiltonian chaos [Lai *et al.*, 1993];
(3) $Q\nabla\Psi \neq 0$ on the attractor, and D is not zero, the system has a strange chaotic attractor. Outside the attractor, the gradient part: $D\nabla\Psi$ determines that the system is dissipative; on the attractor, the system has conserved dynamics, as a result of nonzero rotation part: $Q\nabla\Psi$.

When $\{\mathbf{x} \,|\, \nabla\Psi(\mathbf{x}) = 0\}$ is not fractal, but has nontrivial structure (at least cannot be embedded in a three-dimensional surface of zero genus), the attractor is not strange anymore. But, as shown in Sec. 7.2, the attractor is still possible to be chaotic, depending on the rotation part: $Q\nabla\Psi$.

To sum up, gradient and rotation parts of the vector field are responsible for the creation of strange attractor and chaotic attractor respectively. Although they are both affected by the geometrical configuration of the potential function Ψ, they represent dissipation and circulation respectively.

8. Conclusion

In the present paper it is shown that potential functions with monotonic properties can be constructed in a continuous dissipative chaotic system with strange attractor. Such potential function is a continuous function in phase space, monotonically decreasing with time and remains constant if and only if the limit set is reached. This definition is a natural restriction of generic dynamics since it is a direct generalization of Lyapunov function and corresponds to the concept of energy.

Potential function defined this way also implies that the dynamics can be decomposed into two parts: a gradient part, dissipating energy potential; and a rotation part, conserving energy potential. The gradient part drives the system towards the attractor while the rotation part perpetuates the system's circular motion on the attractor.

To demonstrate the power of this framework in chaotic systems, we simplify the geometric Lorenz attractor, and prove by definition that it is a chaotic attractor. We analytically and explicitly construct a suitable potential function for the attractor, which, to our best knowledge, is the first example in chaotic dynamics. The potential function reveals the fractal nature of the chaotic strange attractor.

We further analyze the concept of chaotic attractor and strange attractor with our decomposition. It is found that chaotic attractor originates in the rotation part, facilitating the state points to

traverse the limit set; while strange attractor originates in the gradient part, causing initial states attracted to the limit set.

Acknowledgments

The authors would like to express their sincere gratitude to Xinan Wang, Ying Tang, Song Xu and Jianghong Shi for their constructive advice throughout this work. The authors also appreciate valuable discussions with James A. Yorke, David Cai, Wei Lin, and Shijun Liao.

This work is supported in part by the Natural Science Foundation of China No. NFSC61073087, the National 973 Projects No. 2010CB529200, and the Natural Science Foundation of China No. NFSC91029738.

References

Anishchenko, V. S. & Strelkova, G. I. [1998] "Irregular attractors," *Discr. Dyn. Nat. Soc.* **2**, 53.

Ao, P. [2004] "Potential in stochastic differential equations: Novel construction," *J. Phys. A*: *Math. Gen.* **37**, 25–30.

Ao, P., Chen, T.-Q. & Shi, J.-H. [2013] "Dynamical decomposition of Markov processes without detailed balance," *Chin. Phys. Lett.* **30**, 070201.

Arnold, V. [1983] *Geometrical Methods in the Theory of Ordinary Differential Equations* (Springer-Verlag, NY).

Arnold, V., Weinstein, A. & Vogtmann, K. [1989] *Mathematical Methods of Classical Mechanics*, 2nd edition (Springer-Verlag, Berlin).

Cheng, D., Spurgeon, S. & Xiang, J. [2000] "On the development of generalized Hamiltonian realizations," *Proc. 39th IEEE Conf. Decision and Control, 2000* (IEEE), pp. 5125–5130.

Freidlin, M. I. & Wentzell, A. D. [1998] *Random Perturbations of Dynamical Systems*, 2nd edition, Grundlehren der Mathematischen Wissenschaften (Springer-Verlag, NY).

Freidlin, M. I. & Wentzell, A. D. [2008] "Some recent results on averaging principle," *Topics in Stochastic Analysis and Nonparametric Estimation*, eds. Chow, P.-L., Yin, G. & Mordukhovich, B. (Springer-Verlag, NY), pp. 1–19.

Gilmore, R. [1998] "Topological analysis of chaotic dynamical systems," *Rev. Mod. Phys.* **70**, 1455–1529.

Grebogi, C., Ott, E., Pelican, S. & Yorke, J. [1984] "Strange attractors that are not chaotic," *Physica D* **13**, 261.

Guckenheimer, J. & Williams, R. F. [1979] "Structural stability of Lorenz attractors," *Publ. Math. IHES* **50**, 59–72.

Guo, Y., Lin, W. & Sanjun, M. A. F. [2012] "The efficiency of a random and fast switch in complex dynamical systems," *New J. Phys.* **14**, 083022.

Kobe, D. H. [1986] "Helmholtz's theorem revisited," *Amer. J. Phys.* **54**, 552–554.

Kuznetsov, S. P. [2012] *Hyperbolic Chaos*: *A Physicist's View* (Springer-Verlag, Berlin, Heidelberg).

Lai, Y.-C., Ding, M. & Grebogi, C. [1993] "Controlling Hamiltonian chaos," *Phys. Rev. E* **47**, 86–92.

Leonov, G. A. & Kuznetsov, N. V. [2007] "Time-varying linearization and the Perron effects," *Int. J. Bifurcation and Chaos* **17**, 1079–1107.

Leonov, G. A. [2008] *Strange Attractors and Classical Stability Theory* (St. Petersburg University Press, St. Petersburg).

Leonov, G. A., Kuznetsov, N. V. & Vagaitsev, V. I. [2011] "Localization of hidden Chua's attractors," *Phys. Lett. A* **375**, 2230–2233.

Leonov, G. A. & Kuznetsov, N. V. [2013] "Hidden attractors in dynamical systems. From hidden oscillations in Hilbert–Kolmogorov, Aizerman, and Kalman problems to hidden chaotic attractor in Chua circuits," *Int. J. Bifurcation and Chaos* **23**, 1330002.

Li, Y., Qian, H. & Yi, Y. [2010] "Nonlinear oscillations and multiscale dynamics in a closed chemical reaction system," *J. Dyn. Diff. Eqs.* **22**, 491–507.

Li, C., Wang, E. & Wang, J. [2012] "Potential flux landscapes determine the global stability of a Lorenz chaotic attractor under intrinsic fluctuations," *J. Chem. Phys.* **136**, 194108.

Liao, S. [2012] "Chaos: A bridge from microscopic uncertainty to macroscopic randomness," *Commun. Nonlin. Sci. Numer. Simulat.* **17**, 2564–2569.

Lorenz, E. N. [1963] "Deterministic nonperiodic flow," *J. Atmosph. Sci.* **20**, 130–141.

Lyapunov, A. M. [1992] "The general problem of the stability of motion," *Int. J. Control* **55**, 531–534.

Ma, Y., Yuan, R., Li, Y., Ao, P. & Yuan, B. [2013] "Lyapunov functions in piecewise linear systems: From fixed point to limit cycle," http://arXiv.org/pdf/1306.6880v1.pdf.

Marsden, J. & McCracken, M. [1976] *Hopf Bifurcation and Its Applications* (Springer).

Olson, J. C. & Ao, P. [2007] "Nonequilibrium approach to Bloch–Peierls–Berry dynamics," *Phys. Rev. B* **75**, 035114.

Peitgen, H.-O., Jürgens, H. & Saupe, D. [2004] *Chaos and Fractals*: *New Frontiers of Science* (Springer-Verlag, NY).

Prasad, A., Nandi, A. & Ramaswamy, R. [2007] "Aperiodic nonchaotic attractors, strange and otherwise," *Int. J. Bifurcation and Chaos* **17**, 3397–3407.

Qian, H. [2013] "A decomposition of irreversible diffusion processes without detailed balance," *J. Math. Phys.* **54**, 053302.

Robinson, C. [1995] *Dynamical Systems*: *Stability*, *Symbolic Dynamics*, *and Chaos* (CRC Press, Boca Raton).

Robinson, R. [2004] *An Introduction to Dynamical Systems*: *Continuous and Discrete* (Pearson Prentice Hall, NJ).

Sabuco, J., Zambrano, S., Sanjun, M. A. & Yorke, J. A. [2012] "Finding safety in partially controllable chaotic systems," *Commun. Nonlin. Sci. Numer. Simulat.* **17**, 4274–4280.

Sarasola, C., d'Anjou, A., Torrealdea, F. J. & Moujahid, A. [2005] "Energy-like functions for some dissipative chaotic systems," *Int. J. Bifurcation and Chaos* **15**, 2507–2521.

Sastry, S. [1999] *Nonlinear Systems*: *Analysis*, *Stability*, *and Control* (Springer-Verlag, NY).

Sira-Ramirez, H. & Cruz-Hernandez, C. [2001] "Synchronizaton of chaotic systems: A generalized Hamiltonian systems approach," *Int. J. Bifurcation and Chaos* **11**, 1381–1395.

Smale, S. [1998] "Mathematical problems for the next century," *Math. Intell.* **20**, 7–15.

Strogatz, S. H. [2001] "Exploring complex networks," *Nature* **410**, 268–276.

Tucker, W. [1999] "The Lorenz attractor exists," *C. R. Acad. Sci. Paris* **328**, 1197–1202.

Vollmer, J., Tél, T. & Breymann, W. [1998] "Entropy balance in the presence of drift and diffusion currents: An elementary chaotic map approach," *Phys. Rev. E* **58**, 1672–1684.

Yuan, R., Ma, Y., Yuan, B. & Ao, P. [2011] "Potential function in dynamical systems and the relation with Lyapunov function," *Proc. 30th Chinese Control Conf. (CCC), 2011* (IEEE), pp. 6573–6580.

Yuan, R. & Ao, P. [2012] "Beyond Itô versus Stratonovich," *J. Stat. Mech.* **2012**, P07010.

Zhou, X. & Weinan, E. [2010] "Study of noise-induced transitions in the Lorenz system using the minimum action method," *Comm. Math. Sci.* **8**, 341–355.

Zhu, X.-M., Yin, L. & Ao, P. [2006] "Limit cycle and conserved dynamics," *Int. J. Mod. Phys. B* **20**, 817–827.

Zinober, A. S. [1994] *Variable Structure and Lyapunov Control* (Springer-Verlag, London).